JACS
JOURNAL OF THE AMERICAN CHEMICAL SOCIETY

Article

pubs.acs.org/JACS

Mesoscale DNA Structural Changes on Binding and Photoreaction with Ru[(TAP)$_2$PHEHAT]$^{2+}$

Willem Vanderlinden,[†] Matthew Blunt,[†] Charlotte C. David,[†] Cécile Moucheron,*[,‡] Andrée Kirsch-De Mesmaeker,*[,‡] and Steven De Feyter*[,†]

[†]Department of Chemistry, Laboratory of Photochemistry and Spectroscopy, Division of Molecular Imaging and Photonics, KU Leuven, Celestijnenlaan 200F, 3001 Leuven, Belgium

[‡]Department of Chemistry, Laboratory of Organic Chemistry and Photochemistry, Université Libre de Bruxelles, Avenue Franklin D. Roosevelt 50, 1050 Brussels, Belgium

Supporting Information

ABSTRACT: We used scanning force microscopy (SFM) to study the binding and excited state reactions of the intercalating photoreagent Ru[(TAP)$_2$PHEHAT]$^{2+}$ (TAP = 1,4,5,8-tetraazaphenanthrene; PHEHAT = 1,10-phenanthrolino[5,6-*b*]1,4,5,8,9,12-hexaazatriphenylene) with DNA. In the ground state, this ruthenium complex combines a strong intercalative binding mode via the PHEHAT ligand, with TAP-mediated hydrogen bonding capabilities. After visible irradiation, SFM imaging of the photoproducts revealed both the structural implications of photocleavages and photoadduct formation. It is found that the rate of photocleaving is strongly increased when the complex can interact with DNA via hydrogen bonding. We demonstrated that the photoadduct increases DNA rigidity, and that the photo-biadduct can crosslink two separate DNA segments in supercoiled DNA. These mechanical and topological effects might have important implications in future therapeutic applications of this type of compounds.

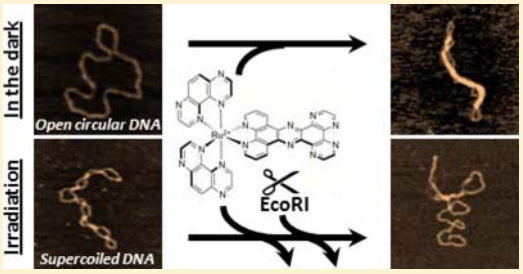

INTRODUCTION

Polyazaaromatic Ru(II) complexes were the focus of numerous researches by virtue of their interesting (photo)electrochemical and photophysical/photochemical properties.[1−6] They led to applications in different fields, for example in biochemistry and biology. In this frame, the studies revealed that these metallic complexes can be used as novel molecular tools or sensors of biomolecules such as DNA[7−16] and could also lead to possible therapeutic agents.[17−19]

Like the well-known anticancer drug Cisplatin, some of these Ru(II) complexes containing a labile ligand can form metallic adducts on DNA by substitution of the labile ligand by a nucleotidic base.[4] More interestingly, other Ru complexes can also be light activated. A considerable amount of research effort has been dedicated to the development of small synthetic ligands exhibiting photoswitchable DNA binding activity.[20,21] The advantage over a dark reactivity is the triggering of the activity upon illumination thus at a chosen time and selected site for the treatment.[10−12,17−19,22,23] Such photoreactions have been possible with Ru complexes that contain at least two TAP (1,4,5,8-tetraazaphenanthrene) ligands. In that case, the excited state being very oxidizing, a photoelectron transfer (PET) process from a guanine (G) base of DNA to the excited complex takes place.[10,25−27] The resulting reduced complex and oxidized G base give rise to either the back electron transfer or adduct formation. The structure of the adduct has been determined and consists of a substitution by a G moiety in the ortho position of the nonchelated nitrogen atom of one of the TAP ligands, at the level of the amino group of this nucleotidic base.[10,17,18,22,27] There is thus no destruction of the chelation sphere around the Ru ion. Such photoadduct formations block enzymes such as RNA polymerase and 3′ exonuclease in in vitro systems.[28−30] Moreover these monoadducts, by absorption of a second photon, and if another G base is in its vicinity, produce the formation of biadducts, thus addition of two G's on the same complex.[31] These processes, when they take place with two G's belonging to either the same strand (single telomeric sequence for instance[32]) or two complementary strands,[31] give rise to an irreversible intra- or inter-photo-crosslinking, respectively. It has also been shown that when these photoreactive complexes are tethered to short (14−17 mer) probe oligonucleotides containing a G in their own sequence (Ru-ODN$_G$), these Ru-ODN$_G$ probes can efficiently photo-crosslink with their target sequences (complementary sequences) provided that the G present on the target strand is located in the vicinity of the complex after hybridization, whereas in the absence of targets, they self-inhibit by intrastrand photoreaction.[33] These processes have been demonstrated to be quite efficient and selective not only in vitro[33] but also with living cells for specific gene silencing in cancerous cells.[34] These Ru complexes are thus interesting and useful compounds. However, in spite of all these experimental data and theoretical calculations to simulate changes of ODN duplex structures by

Received: March 30, 2012
Published: June 5, 2012

   dx.doi.org/10.1021/ja303091q | *J. Am. Chem. Soc.* 2012, 134, 10214−10221

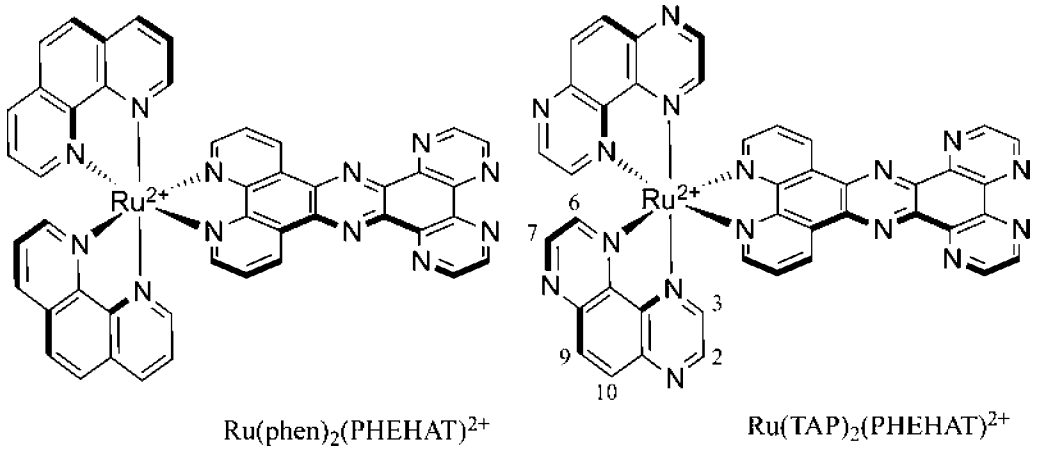

Figure 1. The two Ru(II) PHEHAT complexes. Note that only the Δ-enantiomers are shown; all experiments were, however, performed with the racemic mixture.

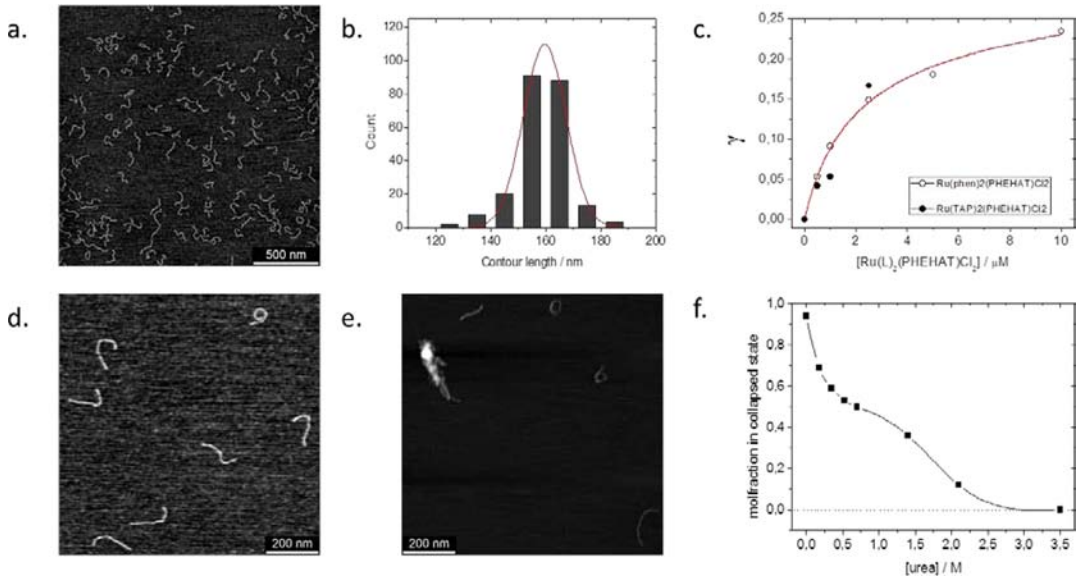

Figure 2. Binding modes of Ru[(phen)$_2$PHEHAT]$^{2+}$ and Ru[(TAP)$_2$PHEHAT]$^{2+}$ to linear DNA. (a–c) Construction of a binding isotherm based on the intercalation-induced lengthening of a 500 base pair restriction fragment: (a) typical SFM topography image of DNA restriction fragments deposited on poly-L-lysine (PLL)-coated mica from Tris buffer containing 7.5 mM Mg(OAc)$_2$ [*z*-range: 1.2 nm]; (b) contour length distribution of the DNA restriction fragments in the absence of complex, fitted to a Gaussian distribution to yield the mean contour length and its standard deviation; (c) fractional occupancy of the DNA, γ, as a function of Ru[(phen)$_2$PHEHAT]$^{2+}$ concentration (open circles) and Ru[(TAP)$_2$PHEHAT]$^{2+}$ concentration (filled circles), where the red line represents the best fit to the data for Ru[(phen)$_2$PHEHAT]$^{2+}$ according to the McGhee and Von Hippel binding theory, yielding intrinsic association constant $K = (1.5 \pm 0.2) \times 10^5$ M^{-1} and site-exclusion number $n = 2.8 \pm 0.3$. (d–f) Hydrogen bonding of TAP leads to DNA structural collapse: (d) SFM topography image of DNA restriction fragments deposited on PLL-coated mica in Tris buffer containing 7.5 mM Mg(OAc)$_2$ and 5 μM Ru[(phen)$_2$PHEHAT]$^{2+}$ [*z*-range: 0.9 nm]; (e) AFM topography image of DNA restriction fragments deposited on PLL-coated mica in Tris buffer containing 7.5 mM Mg(OAc)$_2$ and 5 μM Ru[(TAP)$_2$PHEHAT]$^{2+}$ [*z*-range: 8 nm]; (f) when DNA restriction fragments are incubated with 5 μM Ru[(TAP)$_2$PHEHAT]$^{2+}$ and increasing concentration of urea, there is a steady decrease in the fraction of collapsed molecules, as judged from SFM topographs (the line connecting the data points serves as aguide to the eye).

photoadducts and photo-crosslinkings, not much is known concerning these structural changes.

As mentioned above, the attractive properties of polyazaaromatic Ru(II) complexes have also been used for sensing biological molecules, thanks to the sensitivity of their luminescence to different microenvironments such as DNA. In this context, one of the best well-known examples is the case of the Ru[(bpy/phen)$_2$dppz]$^{2+}$ complex (bpy = 2,2′-bipyridine; phen = 1,10-phenanthroline; dppz = dipyrido[2,3-*a*:3′,2′-*c*]phenazine), which does not luminesce in water but has its emission switched on by intercalation in DNA.[35−37] The Ru[(phen)$_2$(PHEHAT)]$^{2+}$ (Figure 1) (PHEHAT = 1,10-phenanthrolino[5,6-*b*]1,4,5,8,9,12-hexaazatriphenylene) exhibits a similar behavior; its luminescence is also switched on by intercalation of the PHEHAT ligand in DNA.[26,38] A related complex based on the PHEHAT, the Ru[(TAP)$_2$PHEHAT]$^{2+}$ (Figure 1), does also intercalate in DNA but in contrast to its equivalent with two phen ligands, behaves as a light-switch off; it does luminesce in water but undergoes an emission quenching by intercalation in DNA.[39] This quenching is due to the PET processes with the G bases and subsequent reactions as described above.

In the present study, we have studied the impact on DNA structure and topology upon the binding and photoreactions

dx.doi.org/10.1021/ja303091q | J. Am. Chem. Soc. 2012, 134, 10214−10221

with these two intercalating PHEHAT complexes. For that purpose, long DNA or plasmid DNA (thus no short ODN probes as discussed above) have been used as a substrate. Previous experiments have clearly shown by gel electrophoresis[40,41] and scanning force microscopy (SFM)[42] that with plasmid DNA, the illumination of the Ru-TAP complexes is accompanied by DNA photocleavage, as detected by transformation of the supercoiled closed circular (cc) forms into open circular (oc) forms and afterward into linear forms. It has been demonstrated that this is also caused by the PET process with the G bases.[40,41] As such, in addition to the back electron transfer and photoadduct formation as mentioned above, a third process corresponding to DNA cleavages has to be taken into account when long or plasmid DNA molecules are used as a substrate.

Here, we employ SFM to characterize with unprecedented details the ground state binding properties and the effects of photoreaction of $Ru[(TAP)_2PHEHAT]^{2+}$ [39] with DNA, and use $Ru[(phen)_2PHEHAT]^{2+}$ as its nonphotoreactive equivalent[38] (Figure 1). SFM is a powerful technique that has been applied successfully to study DNA and its interactions with proteins and small molecules at the single-molecule level, revealing changes in the DNA geometry and apparent mechanical properties upon ligand binding in a multiplexed fashion.[43−46] Moreover, several publications have appeared on the examination of DNA damage using SFM.[42,47−55] In this study, we find, besides a strong intercalative binding, an unexpected new binding mode that is mediated by TAP ligands. Furthermore, SFM imaging of the "Ru complex/DNA" photoproducts reveals in addition to photocleavages, some DNA structural changes attributed to formation of photoadducts and for longer irradiation times, occurrence of covalent crosslinks between double stranded DNA segments in the case of $Ru[(TAP)_2PHEHAT]^{2+}$. Interestingly, the outcome of the excited state reaction with DNA is affected by the unforeseen ground state binding properties.

RESULTS

DNA Binding Properties: PHEHAT-Mediated Intercalation and Hydrogen Bonding by TAP. First, we aimed at characterizing the ability of $Ru[(phen)_2PHEHAT]^{2+}$ and $Ru[(TAP)_2PHEHAT]^{2+}$ to intercalate in DNA, as deduced from luminescence experiments[38,39] by employing SFM on DNA restriction fragments. It is known that, to accommodate an intercalator, the DNA unwinds and elongates locally. As the distance between the intercalating molecule and the adjacent bases is roughly the same as that between the double-helix base pairs, it is possible to construct a binding-isotherm from the concentration-dependent increase in DNA contour length.[46] The latter value can be obtained from SFM images by measuring the total length of the DNA molecule along its helical axis. In our experiments, different samples were prepared containing varying concentrations of intercalator and for all of these samples around 250 molecules were analyzed in terms of their contour length. A comparison of the intercalator concentration-dependent contour length with the case of zero intercalator concentration allows one to calculate the DNA fractional occupancy γ, i.e., the ratio of bound Ru-intercalator per number of base pairs (see the SI, Materials and Methods).

Figure 2c shows such binding isotherms based on the measurements (Figure 2a,b,d) of the contour lengths of 500 bp restriction fragments, induced by increasing concentrations of the two Ru(II) intercalators. The binding isotherm for $Ru[(phen)_2PHEHAT]^{2+}$ is well described by the ligand binding theory with site-exclusion according to McGhee and Von Hippel.[56] The intrinsic association constant is found to be $(1.5 \pm 0.2) \times 10^5\ M^{-1}$, with a site exclusion factor of 2.8 ± 0.3. This means that binding saturates when the Ru complex is intercalated approximately every three base pairs, in good accordance with previously obtained values for similar complexes, measured with optical and force spectroscopy techniques,[57] as well as SFM imaging.[44]

For $Ru[(TAP)_2PHEHAT]^{2+}$ an unexpected collapse of the DNA structure at 1−5 μM Ru(II) hindered proper fitting of the data to the McGhee and Von Hippel binding theory. At 5 μM $Ru[(TAP)_2PHEHAT]^{2+}$ concentration, most 500 bp restriction fragments seem to have folded back onto themselves, yielding linear and circular fragments of about half the DNA contour length (Figure 2e). A significant number of the DNA molecules were also seen as part of a large intermolecular aggregate. A similar collapse was not observed in the presence of $Ru[(phen)_2PHEHAT]^{2+}$ (Figure 2d), even at higher concentrations, hinting at the influence of the nitrogen atoms at positions 1 and 8 in TAP ligands.

Two mechanisms were evaluated as an explanation for these observations:

(1) TAP might be able to intercalate in between the base pairs of a DNA segment distant from the PHEHAT-intercalation site. Very recently, a cocrystal structure of $Ru[(TAP)_2dppz]^{2+}$ with an oligodeoxynucleotide was published,[58] demonstrating the capability of one of the TAP ligands to bind the DNA by semi-intercalation. However, a quasi-identical geometry was observed in a similar cocrystal structure with $Ru[(phen)_2dppz]^{2+}$.[59] As such, a possible semi-intercalative binding mode seems unable to explain the difference between $Ru[(phen)_2PHEHAT]^{2+}$ and $Ru[(TAP)_2PHEHAT]^{2+}$ observed in vitro.

(2) Another possible interaction type is hydrogen bonding. Indeed, the nitrogen at positions 1 and 8 of the TAP can act as a hydrogen bond acceptor, while hydrogen bond donors might be found in both the major and the minor grooves of the double helix of a distant DNA segment.

To explore the possible role of hydrogen bonding, urea, a strong hydrogen bond donor, was added to the mixture in different concentrations. Adding urea effectively reduced the fraction of collapsed DNA, and at 3.5 M urea, such structures were no longer found (Figure 2f and in the SI Figure S2d, see further). Importantly, the presence of urea did not seem to affect the ability of the complex to intercalate via PHEHAT (Figure S3, SI), neither did it significantly affect the luminescence quantum yield (Figure S4, SI). As such, neither the PHEHAT−DNA interaction nor the metal−ligand coordination seems to be affected. These results support the hypothesis that the observed collapse is mediated by hydrogen bonds.

It should be noted that in principle, also phen might be able to hydrogen bond with DNA or solvent molecules in the aqueous milieu. These hydrogen bonds might then be mediated via C−H moieties or via the π-electron cloud of the aromatic system. However, because of their relatively weak strength and because of the presence of the same hydrogen bond donors/acceptors in TAP, we believe that these weak interactions have limited significance (see the Supporting Information) and do not explain the marked differences for TAP as compared to phen described above.

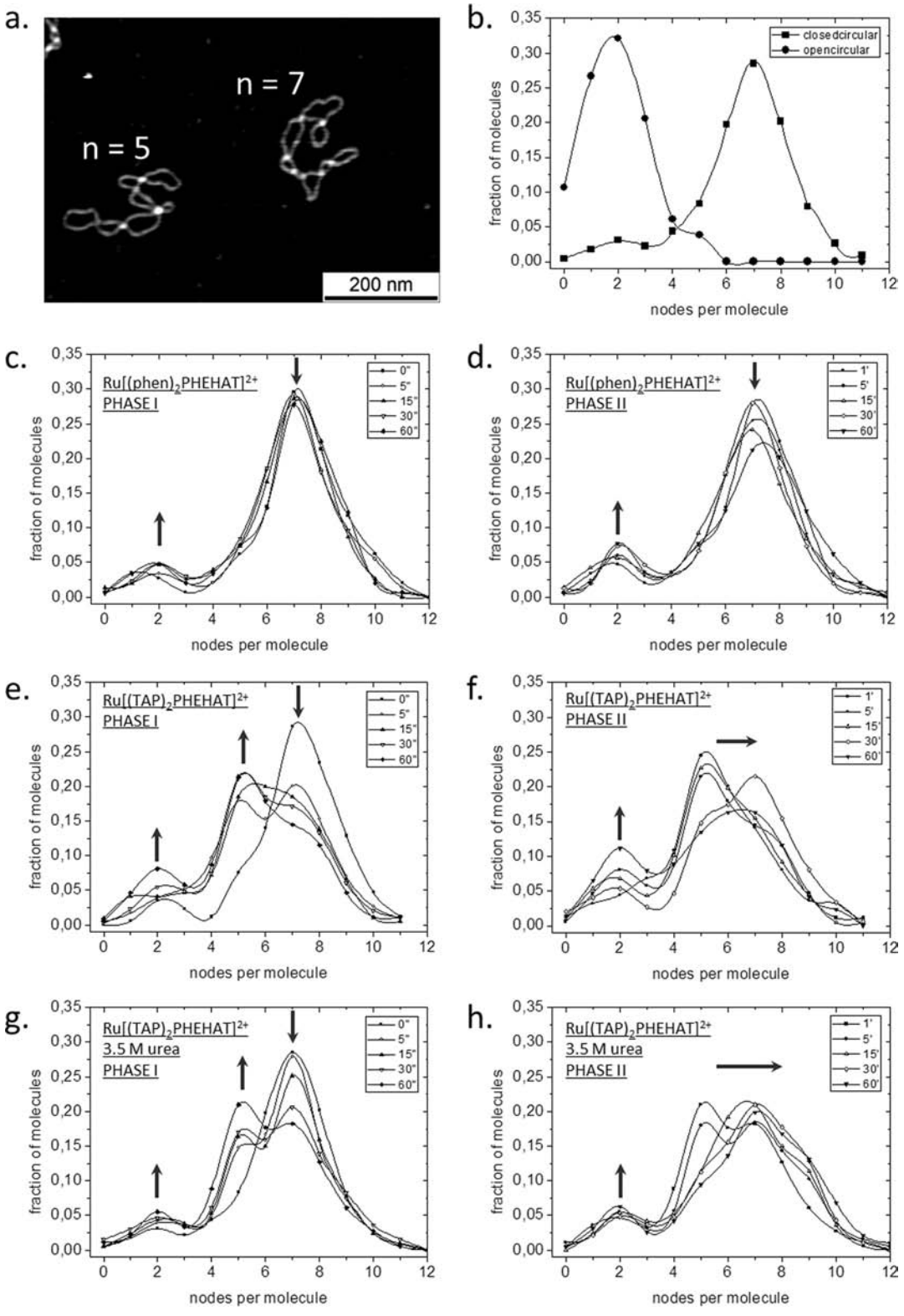

Figure 3. SFM analysis of the products resulting from the irradiation resolves nicking activity and photoadduct formation. (a) SFM topograph of two plasmids deposited on PLL-coated mica, with indicated node numbers "*n*". (b) Demonstration of the resolution of closed circular and open circular plasmid molecules. (c–h) Node number distribution as a function of irradiation time: for $Ru[(phen)_2PHEHAT]^{2+}$ (c: 0–60 s irradiation time; d: 1–60 min irradiation time), for $Ru[(TAP)_2PHEHAT]^{2+}$ in the absence of urea (e: 0–60 s irradiation time; f: 1–60 min irradiation time), and for $Ru[(TAP)_2PHEHAT]^{2+}$ in the presence of 3.5 M urea (g: 0–60 s irradiation time; h: 1–60 min irradiation time).

SFM Reveals Mechanical and Topological Changes in $Ru[(TAP)_2PHEHAT]^{2+}$-Photosensitized DNA. In the next step, we address the impact of the photoreaction sensitized by $Ru[(TAP)_2PHEHAT]^{2+}$ on the mesoscale structure of supercoiled plasmid DNA molecules. High-affinity DNA binding via intercalation, as quantified in the previous section, has increased

dx.doi.org/10.1021/ja303091q | J. Am. Chem. Soc. 2012, 134, 10214–10221

the yield of lesions formed by second generation cisplatin derivatives.[60] In contrast to these Pt compounds, Ru[(TAP)$_2$PHEHAT]$^{2+}$ can form under illumination covalent adducts with DNA via the TAP ligand (see the Introduction). Moreover, early experiments on the light-reaction between ruthenium−TAP complexes with supercoiled plasmid DNA have indicated the efficient formation of nicks in the DNA backbone via photo-oxidation.[40−42] Here we use SFM to investigate the effect of irradiating supercoiled plasmids in the presence of Ru[(TAP)$_2$PHEHAT]$^{2+}$. More specifically, supercoiled pUC19 plasmids (0.5 mg/L) were mixed with 10 nM Ru[(TAP)$_2$PHEHAT]$^{2+}$ in the presence of 7.5 mM $Mg^{2+}$and irradiated at 445 nm for several irradiation times. These samples were then subjected to an extensive dialysis against Tris-HCl buffer to remove free Ru[(TAP)$_2$PHEHAT]$^{2+}$ and buffer salts. After adjustment to the original salt conditions (10 mM Tris-HCl, 7.5 mM $Mg(OAc)_2$, pH 8) the photoproducts were deposited onto PLL-coated mica and analyzed by SFM. We have extended the approach used by Jiang et al. to characterize the DNA damage after irradiation.[47] These authors have used SFM to detect the geometrical changes induced by single strand breaks in plasmids generated during irradiation in solution. As a substrate, they used a mica surface that was modified such that the DNA was kinetically trapped upon adsorption. In this case, the plectonemic conformation of intact, supercoiled plasmids is maintained on the surface, resulting in multiple intramolecular overlaps (or nodes). Nicked molecules adopt an open circular conformation in solution, and adsorb on this type of surface in a conformation without or with very few nodes. Quantitative characterization of the node numbers in reference samples allowed them to annotate a given plasmid as intact or damaged based on the node number for this particular molecule. We adopted this approach in this study, but took it one step further by quantifying the molar fraction of molecules with different node numbers for every irradiation time.

First we confirmed the capability of the technique to resolve nicked circular from supercoiled pUC19 DNA molecules. To do so, we compared enzymatically nicked plasmids with untreated ones (Figure 3b). The enzymatically nicked plasmids appear in a largely open conformation on the surface, and quantification results in a single peak centered on a node number of 2. Untreated plasmid molecules appear mainly in a supercoiled conformation, with a mean node number of 7, while a smaller fraction (5−10%) of the sample shows up in the peak centered at a node number of 2, reflecting the amount of damaged DNA during extraction and purification.

Next, we examined the products of the photoreaction sensitized by a small amount (10 nM) of Ru[(phen)$_2$PHEHAT]$^{2+}$. The molecular ensembles can be well described by a bimodal node number distribution, irrespective of the irradiation time (Figure 3c,d). A global fitting analysis using the sum of two gaussians and integration of respective peaks quantifies the time-resolved photocleaving activity (Figure S6, SI). An important observation is the offset fraction of plasmids that is not cleaved at all. A possible explanation is a cooperative binding mechanism, which at these low complex-to-DNA ratios might result in a fraction of DNA molecules that is virtually without complex intercalation.

Given the successful validation of the experimental approach, the photoproducts formed in the presence of Ru[(TAP)$_2$PHEHAT]$^{2+}$ were subsequently analyzed. A decrease of the fraction of supercoiled molecules (i.e., the peak centered at node number 7) and an increase of the molecular fraction of nicked plasmids (i.e., the peak centered at node number 2) is observed (Figure 3e,f). However, the fraction of molecules with an intermediate number of nodes increases unexpectedly during the first minute of irradiation (phase I). Longer irradiation times reverse this effect, again yielding higher node numbers (phase II). We attribute this striking two-phase behavior as the result of the formation of covalent adducts between the complex and the DNA. This hypothesis is supported by the comparison of our observations with the effects of Ru[(phen)$_2$PHEHAT]$^{2+}$ (vide supra). For short as well as for longer irradiation times, there is no deviation from a bimodal node number distribution. As already shown, Ru[(phen)$_2$PHEHAT]$^{2+}$ is not sufficiently oxidizing in its excited state to directly oxidize a DNA, and as such cannot form a covalent adduct. It behaves as a classical sensitizer for DNA photocleavage.

To find the molecular principles underlying the observed trends in irradiated circular DNA molecules, additional experiments were undertaken. In an attempt to explain the shift of supercoiled molecules toward lower node numbers (in the first phase) linear 500 bp DNA restriction fragments were irradiated in the presence of Ru[(TAP)$_2$PHEHAT]$^{2+}$. SFM imaging of the photoproducts reveals an obvious increase in the end-to-end distance (Figure 4). The contour length, however,

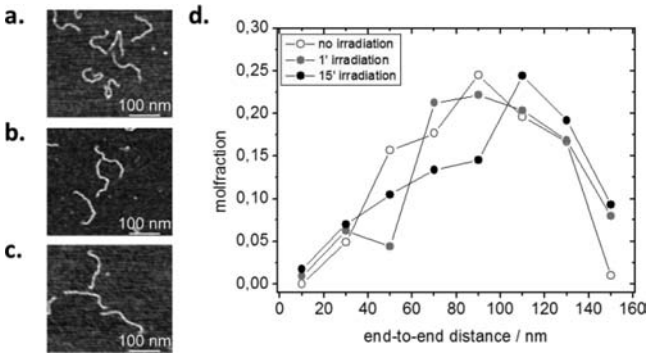

Figure 4. Impact of the monoadduct on DNA mechanics. SFM analysis of 500 bp linear DNA fragments (a) before irradiation, (b) after 1 min of irradiation in the presence of 10 nM Ru[(TAP)$_2$PHEHAT]$^{2+}$, and (c) after 15 min of irradiation in the presence of 10 nM Ru[(TAP)$_2$PHEHAT]$^{2+}$, and (d) distribution of end-to-end distances for 500 bp restriction fragments after different irradiation times.

remains unchanged (Figure S7, SI), and thus one can conclude that the DNA's resistance to bending has increased. This might well explain the observed trend toward lower node numbers (phase I) in irradiated DNA circles. Indeed, an increased persistence to bending would result in a globally more open conformation of the supercoiled molecule.

It must be noted that a reduction of the bending persistence at longer irradiation time should be discarded as a possible explanation for the increase in node number: after an irradiation time of 15 min, the end-to-end distance of the 500 bp DNA restriction fragments has not decreased. However, as Ru complexes containing at least two TAP ligands are capable of forming an interstrand crosslink between two guanine units present in two complementary oligodeoxyribonucleotides,[31] a similar photo-crosslinking might occur between two guanine bases located on different DNA segments on the same plasmid. In such a case, a new topological domain would be introduced in a plasmid, resulting in an increased node

number. To test this hypothesis, supercoiled pUC19 sample with the Ru complex was irradiated (60 min irradiation time), dialyzed, and subsequently digested by the *Eco*RI restriction enzyme, which recognizes a single site in the pUC19 sequence. In the case that the irradiation step is omitted, enzymatic restriction results in completely relaxed, linearized plasmids (Figure 5a). However, if a photo-crosslinking event between

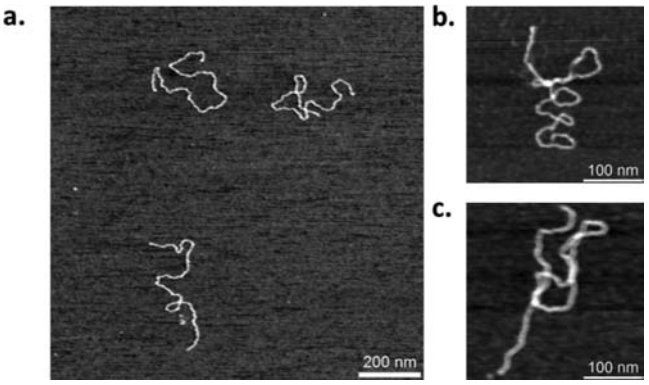

Figure 5. Impact of intersegmental biadducts on DNA topology. Effect of plasmid linearization (a) on nonirradiated samples and (b, c) on samples dialyzed after 60 min of irradiation in the presence of 10 nM $Ru[(TAP)_2PHEHAT]^{2+}$ and 3.5 M urea.

two chemically distant sites has divided the plasmid into two separated topological domains, the linearization by the enzyme should result in only a partial relief of the supercoiling. The unaffected topological domain would in other words still remain supercoiled. The discovery of linearized plasmids with an internal, supercoiled domain effectively confirms this presumption (Figure 5b,c). It should be noted that a very similar approach has recently been used to show that certain proteins are capable of dividing a plasmid molecule into two topological domains.[61]

Hydrogen Bonding Mediated by TAP Influences the Photocleavages, but Not the Photoadducts Formation. The effect of intercalation on the outcome of the photoreaction has recently been studied by using oligodeoxyribonucleotides tethered to a $Ru[(TAP)_2dppz]^{2+}$ via a flexible linker.[62] When the complex is linked via a TAP moiety, the high-affinity binding of $Ru[(TAP)_2dppz]^{2+}$ via dppz intercalation increases the PET efficiency as compared to the nonintercalative binding mode. However, the resulting oxidized guanine is subsequently less likely to form an adduct with reduced $Ru[(TAP)_2dppz]^{+}$, as compared to the situation where the complex is linked via the dppz ligand and DNA bound via the TAP ligands. Very likely, this effect arises from the reduced conformational flexibility when the complex is locked in its intercalation-binding site.

Given the hydrogen bonding mediated by TAP, it is of interest to examine its effect on the outcome of the photoreaction in the presence of supercoiled pUC19. To do so, SFM was employed to study the photo-oxidation of supercoiled pUC19 by $Ru[(TAP)_2PHEHAT]^{2+}$ in the presence of 3.5 M urea. This should selectively break the TAP-mediated hydrogen bonding with DNA as shown above. Preliminary controls indicated that the presence of 3.5 M urea does not affect intercalation via PHEHAT, the double-stranded DNA structure, nor the luminescence quantum yield of $Ru[(TAP)_2PHEHAT]^{2+}$ (Figures S3 and S4, SI) .

Parts g and h of Figure 3 show the node number distributions of the pUC19 photoproducts as a function of illumination time. Similar to the products irradiated in the absence of urea, there are deviations from the effects of a classical photosensitizer. Very similar trends compared to the situation without urea are observed; however, a feature clearly distinct is the nicking rate. In the presence of 3.5 M urea, photocleavage is dramatically decreased. This was confirmed by using agarose gel electrophoresis (Figure S5, SI). This technique allowed resolving two bands, reflecting the open circular form and the supercoiled form. No nicking activity was observed when the samples were irradiated in the presence of 3.5 M urea, as compared to the standard samples lacking urea. We conclude that the photocleaving activity of $Ru[(TAP)_2PHEHAT]^{2+}$ is increased by ground state hydrogen bonding, while adduct formation is not significantly affected.

CONCLUSION

We have examined the binding properties of $Ru[(phen)_2PHEHAT]^{2+}$ and $Ru[(TAP)_2PHEHAT]^{2+}$ to DNA. Both complexes are shown to have a strong affinity for DNA, due to their intercalating properties. $Ru[(TAP)_2PHEHAT]^{2+}$ was additionally seen to crosslink DNA segments in the dark, in contrast to $Ru[(phen)_2PHEHAT]^{2+}$. This behavior cannot be explained via a semi-intercalative binding mode, as observed recently in a DNA–$Ru[(TAP)_2dppz]^{2+}$ cocrystal structure. Indeed, in the crystal, $Ru[(phen)_2dppz]^{2+}$ behaves quasi-identically compared to its TAP-containing counterpart. Very likely, in solution additional/different DNA-binding modes of TAP may be present. We provided evidence that TAP is able to form hydrogen bonds, very likely employing the nitrogens at positions 1 and 8 in the TAP moieties as hydrogen bond acceptors. We demonstrated that there is a relationship between the possibility to form hydrogen bonds, and the excited state dynamics.

A detailed analysis of irradiated samples allowed us to study the evolution of the DNA structural changes over time (Figure 6). More specifically, we were able to observe simultaneously the formation of single strand breaks and the formation of covalent adducts in biologically relevant supercoiled plasmid DNA upon visible light irradiation. The induction of single-strand breaks removes the torsional constraints in the plasmid and transforms the supercoiled molecule into an open circle. Photoinduced mono- and biadducts affect the structure of the supercoiled DNA in a complex manner. This behavior seems to originate from both mechanical and topological changes in the DNA upon irradiation: DNA bending flexibility is reduced by monoadducts and maybe intrasegmental biadduct formation, and intersegmental biadducts can covalently crosslink different DNA segments.

Interestingly, the nicking activity is strongly decreased when TAP–DNA hydrogen bonding is prevented by urea, while this seems not to have an effect on the formation of adducts. At this point the origins of the increased photocleaving activity in the absence of urea are not clear. However, it seems that the photocleavages benefit from a specific DNA–TAP geometry and that this geometry is achieved (at least to a certain extent) via TAP–DNA hydrogen bonding.

The hydrogen bonding capability is expected not to be exclusive for $Ru[(TAP)_2PHEHAT]^{2+}$, but might be an important factor in other TAP-containing compounds. Similar to certain minor-groove binders and DNA-binding proteins, such hydrogen bonding might occur in the grooves of the DNA

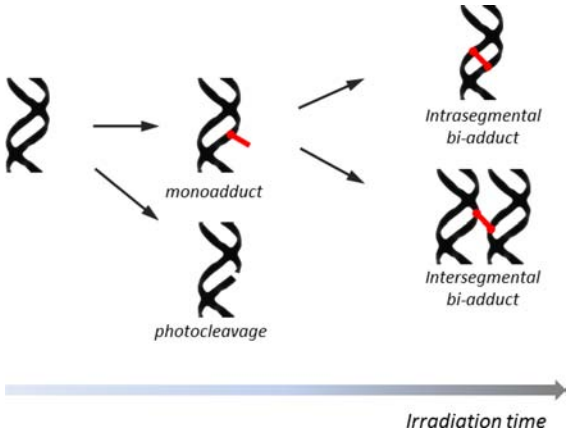

Figure 6. Schematic representation of the photoreactions of $Ru[(TAP)_2PHEHAT]^{2+}$ with DNA. Using supercoiled plasmids as a substrate, we can directly observe DNA photocleaving via SFM imaging. In this case, the open circular form can be distinguished from the supercoiled closed circular form on the basis of the large difference in the node numbers for these two forms. The effect of the monoadduct—probably combined with the effect of local, intrasegmental biadducts—is to reduce the number of nodes observed in supercoiled plasmids via an increased bending rigidity. At longer irradiation times, the node numbers of the supercoiled plasmids again increase, to values above those for untreated plasmids. This is shown to be the consequence of DNA photo-crosslinking via the formation of intersegmental biadducts.

and infer a certain degree of sequence specificity or selectivity. This might be of interest in the rational design of optimized photoprobes. Moreover, as outlined above, we showed that adduct and biadduct formation increases the DNA stiffness, and leads to formation of crosslinks between different segments of the DNA. Thus from these mechanical and topological effects of the covalently bound adducts, in addition to their local action as a molecular "roadblock" for processive enzymes,[28,29] important cellular implications might be expected.

■ ASSOCIATED CONTENT

Supporting Information

Materials and Methods section and details on the following topics: DNA adsorption on poly-L-lysine coated mica to exclude effects of sample preparation; intramolecular collapse of open circular DNA induced by $Ru[(TAP)_2PHEHAT]^{2+}$; possible hydrogen bonding patterns mediated by phen have limited significance; hydrogen bond formation stimulates DNA photocleaving as shown by gel electrophoresis; SFM quantifies photosensitization by $Ru[(phen)_2PHEHAT]^{2+}$; and adduct formation does not affect DNA contour length. This material is available free of charge via the Internet at http://pubs.acs.org.

■ AUTHOR INFORMATION

Corresponding Author

*cmouche@ulb.ac.be; akirsch@ulb.ac.be; Steven.DeFeyter@chem.kuleuven.be

Notes

The authors declare no competing financial interest.

■ ACKNOWLEDGMENTS

The research leading to these results has received funding from the Fund of Scientific Research–Flanders (FWO), the Belgian National Science Foundation (FNRS), KU Leuven (GOA), the Belgian Federal Science Policy Office through IAP-6/27, the Institute for the Promotion of Innovation by Science and Technology in Flanders (IWT), and the European Cooperation in Science and Technology (COST).

■ REFERENCES

(1) Juris, A.; Balzani, V.; Barigelletti, F.; Campagna, S.; Belser, P.; von Zelewsky, A. *Coord. Chem. Rev.* **1988**, *84*, 85–277.
(2) Balzani, V.; Juris, A.; Venturi, M.; Campagna, S.; Serroni, S. *Chem. Rev.* **1996**, *96*, 759–833.
(3) Daniel, C. *Coord. Chem. Rev.* **2003**, 238–239.
(4) Vos, J. G.; Kelly, J. M. *Dalton Trans.* **2006**, *41*, 4869–4883.
(5) Vlček, A., Jr.; Záliš, S. *Coord. Chem. Rev.* **2007**, *251*, 258–287.
(6) Campagna, S.; Puntoriero, F.; Nastasi, F.; Bergamini, G.; Balzani, V. *Top. Curr. Chem.* **2007**, *280*, 117–214.
(7) Erkkila, K. E.; Odom, D. T.; Barton, J. K. *Chem. Rev.* **1999**, *99*, 2777–2795.
(8) Nordén, B.; Lincoln, P.; Akerman, B.; Tuite, E. *Met. Ions Biol. Syst.* **1996**, *33*, 177–252.
(9) Moucheron, C.; Kirsch-De Mesmaeker, A.; Kelly, J. M. *Struct. Bonding (Berlin)* **1998**, *92*, 163–216.
(10) Elias, B.; Kirsch-De Mesmaeker, A. *Coord. Chem. Rev.* **2006**, *250*, 1627–1641.
(11) Ortmans, I.; Moucheron, C.; Kirsch-De Mesmaeker, A. *Coord. Chem. Rev.* **1998**, *168*, 233–271.
(12) Herman, L.; Ghosh, S.; Defrancq, E.; Kirsch-De Mesmaeker, A. *J. Phys. Org. Chem.* **2008**, *21*, 670–681.
(13) Pisani, M. J.; Fromm, P. D.; Mulyana, Y.; Clarke, R. J.; Korner, H.; Heimann, K.; Collins, J. G.; Keene, F. R. *ChemMedChem* **2011**, *6*, 848–858.
(14) Tian, X. H.; Gill, M. R.; Canton, I.; Thomas, J. A.; Battaglia, G. *ChemBioChem.* **2011**, *12*, 548–541.
(15) Jimenez-Hernandez, M. E.; Orellana, G.; Montero, F.; Portoles, M. T. *Photochem. Photobiol.* **2000**, *72*, 28–34.
(16) Önfelt, B.; Gostring, L.; Lincoln, P.; Nordén, B.; Önfelt, A. *Mutagenesis* **2002**, *17*, 317–320.
(17) Schatzschneider, U.; Niesel, J.; Ott, I.; Gust, R.; Alborzinia, H.; Wölfl, S. *ChemMedChem* **2008**, *3*, 1104–1109.
(18) Ghesquière, J.; Le Gac, S.; Marcélis, L.; Moucheron, C.; Kirsch-De Mesmaeker, A. *Curr. Top. Med. Chem.* **2012**, *18*, 355–364.
(19) Clarke, M. J. *Coord. Chem. Rev.* **2002**, *232*, 69–93.
(20) Di Pietro, M. L.; Puntoriero, F.; Tuyéras, F.; Ochsenbein, P.; Lainé, P. P.; Campagna, S. *Chem. Commun.* **2010**, *46* (28), 5169–5171.
(21) Andersson, J.; Li, S.; Lincoln, P.; Andréasson, J. *J. Am. Chem. Soc.* **2008**, *130* (36), 11836–11837.
(22) Moucheron, C. *New J. Chem.* **2009**, *33*, 235–245.
(23) Rademaker-Lakhai, J.; van den Bongard, D.; Pluim, D.; Beijnen, J. H.; Schellens, J. H. M. *Clin. Cancer Res.* **2004**, *10*, 3717–3727.
(24) Levina, A.; Mitra, A.; Lay, P. A. *Metallomics* **2009**, *1*, 458–470.
(25) Moucheron, C.; Kirsch-De Mesmaeker, A.; Kelly, J. M. *J. Photochem. Photobiol. B* **1997**, *40*, 91–106.
(26) Kirsch-De Mesmaeker, A.; Moucheron, C.; Boutonnet, N. *J. Phys. Org. Chem.* **1998**, *11*, 566–576.
(27) Jacquet, L.; Kelly, J. M.; Kirsch-De Mesmaeker, A. *Chem. Commun.* **1995**, 913–914.
(28) Pauly, M.; Kayser, I.; Schmitz, M.; Dicato, M.; Del Guerzo, A.; Kolber, I.; Moucheron, C.; Kirsch-De Mesmaeker, A. *Chem. Commun.* **2002**, 11086–1087.
(29) Lentzen, O.; Constant, J. F.; Defrancq, E.; Prevost, M.; Schumm, S.; Moucheron, C.; Dumy, P.; Kirsch-De Mesmaeker, A. *ChemBioChem* **2003**, *4*, 195–202.
(30) Lentzen, O.; Defrancq, E.; Constant, J. F.; Schumm, S.; Garcia-Fresnadillo, D.; Moucheron, C.; Dumy, P.; Kirsch-De Mesmaeker, A. *J. Biol. Inorg. Chem.* **2004**, *9*, 100–108.
(31) Ghisdavu, L.; Pierard, F.; Rickling, S.; Aury, S.; Surin, M.; Beljonne, D.; Lazzaroni, R.; Murat, P.; Defrancq, E.; Moucheron, C; Kirsch-De Mesmaeker, A. *Inorg. Chem.* **2009**, *48*, 10988–10994.

(32) Rickling, S.; Ghisdavu, L.; Pierard, F.; Gerbaux, P.; Surin, M.; Defrancq, E.; Moucheron, C.; Kirsch-De Mesmaeker, A. *Chem.—Eur. J.* **2010**, *16*, 3951−3961.
(33) Le Gac, S.; Rickling, S.; Gerbaux, P.; Defrancq, E.; Moucheron, C.; Kirsch-De Mesmaeker, A. *Angew. Chem., Int. Ed.* **2009**, *48*, 1122−1125.
(34) Reschner, A.; Bontems, S.; Le Gac, S.; Lambermont, J.; Marcélis, L.; Defrancq, E.; Hubert, P.; Moucheron, C.; Kirsch-De Mesmaeker, A.; Raes, M.; Piette, J.; Delvenne, P. *Gene Ther.*, submitted for publication.
(35) Friedman, A. E.; Chambron, J. C.; Sauvage, J. P.; Turro, N. J.; Barton, J. K. *J. Am. Chem. Soc.* **1990**, *112*, 4960−4962.
(36) Olson, E. J. C.; Hu, D.; Hörmann, A.; Jonkman, A. M.; Arkin, M. R.; Stemp, E. D. A.; Barton, J. K.; Barbara, P. F. *J. Am. Chem. Soc.* **1997**, *119*, 11458−11467.
(37) McKinley, A. W.; Lincoln, P.; Tuite, E. M. *Coord. Chem. Rev.* **2011**, *255*, 2676−2692.
(38) Moucheron, C.; Kirsch-De Mesmaeker, A.; Choua, S. *Inorg. Chem.* **1997**, *36*, 584−592.
(39) Moucheron, C.; Kirsch- De Mesmaeker, A. *J. Phys. Org. Chem.* **1998**, *11*, 577−583.
(40) Kelly, J. M.; Feeney, M. M.; Tossi, A. B.; Lecomte, J.-P.; Kirsch-De Mesmaeker, A. *Anti-Cancer Drug Des.* **1990**, *5*, 69−75.
(41) Kelly, J. M.; McConnell, D. J.; OhUigin, C.; Tossi, A. B.; Kirsch-De Mesmaeker, A.; Masschelein, A.; Nasielski, J. *Chem. Commun.* **1987**, 1821−1823.
(42) Uji-i, H.; Foubert, P.; De Schryver, F. C.; De Feyter, S.; Gicquel, E.; Etoc, A.; Moucheron, C.; Kirsch-De Mesmaeker, A. *Chem.—Eur. J.* **2006**, *12*, 758−762.
(43) Bustamante, C.; Rivetti, C. *Annu. Rev. Biophys. Biomol. Struct.* **1996**, *25*, 395−429.
(44) Mihailovic, A.; Vladescu, I.; McCauley, M.; Ly, E.; Williams, M. C.; Spain, E. M.; Nuñez, M. E. *Langmuir* **2006**, *22*, 4699−4709.
(45) Hou, X. M.; Zhang, X. H.; Wei, K. J.; Ji, C.; Dou, S. X.; Wang, W. C.; Li, M.; Wang, P. Y. *Nucleic Acid Res.* **2009**, *37*, 1400−1410.
(46) Coury, J. E.; McFail-Isom, L.; Williams, L. D.; Bottomley, L. A. *Proc. Natl. Acad. Sci. U.S.A.* **1996**, *93*, 12283−12286.
(47) Jiang, Y.; Ke, C.; Mieczkowski, P. A.; Marszalek, P. E. *Biophys. J.* **2007**, *93*, 1758−1767.
(48) Su, M.; Yang, Y.; Yang, G. *FEBS Lett.* **2006**, *580* (17), 4136−42.
(49) Yoshikawa, Y.; Hizume, K.; Oda, Y.; Takeyasu, K.; Araki, S.; Yoshikawa, K. *Biophys. J.* **2006**, *90*, 993−9.
(50) Piétrement, O.; Pastré, D.; Landousy, F.; David, M. O.; Fusil, S.; Hamon, L.; Zozime, A.; Le Cam, E. *Eur. Biophys. J.* **2005**, *34*, 200−7.
(51) Boichot, S.; Fromm, M.; Cunniffe, S.; O'Neill, P.; Labrune, J. C.; Chambaudet, A.; Delain, E.; Le Cam, E. *Radiat. Prot. Dosim.* **2002**, *99*, 143−145.
(52) Psonka, K.; Brons, S.; Heiss, M.; Gudowska-Nowak, E.; Taucher-Scholz, G. *J. Phys.: Condens. Matter* **2005**, *17*, S1443−S1446.
(53) Murakami, M.; Hirokawa, H.; Hayata, I. *J. Biochem. Biophys. Methods* **2000**, *44*, 31−40.
(54) Pang, D.; Berman, B. L.; Chasovskikh, S.; Rodgers, J. E.; Dritschilo, A. *J. Radiat. Res.* **1998**, *150*, 612−618.
(55) Pang, D.; Rodgers, J. E.; Berman, B. L.; Chasovskikh, S.; Dritschilo, A. *J. Radiat. Res.* **2005**, *164*, 755−765.
(56) McGhee, J. D.; Von Hippel, P. H. *J. Mol. Biol.* **1974**, *86*, 469−489.
(57) Vladsecu, I. D.; McCauley, M. J.; Nunez, M. E.; Rouzina, I.; Williams, M. C. *Nat. Methods* **2007**, *4*, 517−522.
(58) Hall, J. P.; O'Sullivan, K.; Nascer, A.; Smith, J. A.; Kelly, J. M.; Cardin, C. J. *Proc. Natl. Acad. Sci. U.S.A.* **2011**, *108*, 17610−17614.
(59) Private communication.
(60) Petitjean., A.; Barton, J. K. *J. Am. Chem. Soc.* **2004**, *126*, 14728−14729.
(61) Leng, F.; Chen, B.; Dunlap, D. D. *Proc. Natl. Acad. Sci. U.S.A.* **2011**, *108*, 19973−19978.
(62) Le Gac, S.; Foucart, M.; Gerbaux, P.; Defrancq, E.; Moucheron, C.; Kirsch-De Mesmaeker, A. *Dalton Trans.* **2010**, *39*, 9672−9683.